# Implementation of FOC based speed control for an E-Rickshaw brushless DC drive

IOP Conf. Series: Materials Science and Engineering **906** (2020) 012026 doi:10.1088/1757-899X/906/1/012026

# Implementation of FOC based speed control for an E-Rickshaw brushless DC drive

**T. J.Prem Prasanna[1], Devavrat Shyam Anikhindi[1], S. Afzal Ahamed[1], B. Ashok[2], R. Raja Singh[3]**

[1]Department of Automotive Engineering, Vellore Institute of Technology, Vellore, India.
[2]School of Mechanical Engineering, Vellore Institute of Technology, Vellore, India.
[3]Advanced Drives Laboratory, Department of Energy & Power Electronics, Vellore Institute of Technology, Vellore, India.
Coorospondance: premprasanna1997@gmail.com

**Abstract**. This paper describes an approach to implement Field Oriented Control (FOC) using PID Controller for a brushless direct control (BLDC) motor. The research proposes reduction in total harmonic distortion of the supply current using space vector pulse width modulation technique. Minimization of total harmonic distortion becomes mandatory for a smooth operation in electric vehicle applications. As the harmonics are generated in the supply current, caused by non-linear load in E-Rickshaw. The lower, the value of total harmonic distortion givers better performance of the motor when operated under light load. Here the different strategies employed for controlling BLDC motor speed is analyzed and compared. It also proved that the space vector pulse width modulation technique improves the reliability due to the balanced switching frequency achieved from the solid-state switches in the inverter. Through simulating, the proposed control strategy is analyzed and compared with the existing techniques results in smooth change in current during sudden loading, which improves system performance and as a result the torque ripple gets minimized. The comparative study was made in the Matlab/Simulink 2019b, by designing the mathematical model of motor, inverter and the switching sequence, and the max-min algorithm for the SVPWM.

## 1. Introduction

Recent years have seen a huge spike in the development of high-performance motor drives. These drives have proven immense importance in a plethora of applications like automotive, computer, steel rolling mills, electric trains, robotics etc.[1], [2]. Common methods for designing industrial speed controllers are experimental, root locus, frequency and optimization methods [3]. A lot of research has been done on speed control of a BLDC motor using a proportional-integral-differential (PID) controller. However, BLDC motors might give rise to large overshoots, slow response times and large steady state error. For these reasons, the gain values of the PID controller need to be tuned to obtain satisfactory output from the motor under varying load and speed conditions.The ziegler-nichols method which is widely used for tuning the PID controller with systems whose plant model can be single input single output systems. But for complex systems like the BLDC motor modeling it cannot be applicable. And as the PID controllers have the following advantages like easier to implement, uses lesser resources, more robust to tuning mismatches and better response to unmeasured disturbances. And the recent methodology for tuning the gains is using fuzzy logic controllers in addition to PID [4], [5], [6]. In this method, the PID controller sends the main control signals in the form of pulse width

modulated (PWM) waves. As a feedback, speed error and change in error are taken into consideration and fuzzified. Then based on pre-set lookup tables, the values of the gains are obtained by the process of defuzzification. The next advancement on tuning the PID controller is by sing adaptive fuzzy controller [7],[8],[9],10]. In this method, in addition to the fuzzy PID control process, an adaptive process of normalizing the inputs and outputs of the fuzzy controller is employed [11]. This puts a cap on the error obtained and provides slightly finer results under certain operating conditions.
There are different types of PWM techniques, among them the SVPWM and SPWM are popularly employed modulation techniques for industrial applications, especially with semiconductor switch converters. Due to the robust nature of the mode of operation at various speeds, the sinusoidal PWM technique is being used [12], [13]. The semiconductor switches that are bring used along with the driver circuit application are Metal-Oxide Semiconductor Field-Effect Transistor (MOSFET), Insulated Gate Bipolar Transistor (IGBT) and Bipolar Junction Transistor (BJT). These switches exhibit continuous drain current property, i.e., generally 80 A at 25°C and it decreases to 65 A at 100°C. Due to this decrease in the continuous drain current property of the switches multiple switches are connected in parallel, this makes the circuit more robust to operate at any operating temperature and is more safe. So, for the motor driver applications generally 6 switches are required to build the convertor. But due to the property of continuous drain current, 12 switches are used. And the pulse wave form from the controller triggers the gates of the switches. When the gate is triggered in a sequence of operation, so that combined operating behavior of all the switches gives the 3 phase AC output to the Motor windings [14]. The BLDC motor and the Permanent Magnet Synchronous Motor (PMSM) both have the permanent magnet rotor and there are 3 stator windings connected in star pattern. But the only difference between the PMSM and the BLDC is interconnection of coils in the stator windings. The PMSM have distributed stator windings (coils spanning more than one tooth) and BLDC have concentrated stator windings (coils wound around each tooth). This makes the back EMF of the PMSM as sinusoidal and for BLDC as Trapezoidal[15]. And while designing the mathematical model of the motor, the back EMF is created using the lookup table based on the position of the motor (degrees of rotation). The BLDC motor stator is made up of stacked steel laminations wherein windings are placed in groups that are axially cut along their inner periphery[16]. Mostly, all the BLDC motor have 3 start connected stator windings. Each winding is constructed with numerous interconnected coils, with one or more coils placed in the stator slot. These windings along with the stator periphery form an even number of poles. This type of winding arrangement in the BLDC motor makes the torque ripple to be higher than the PMSM motor. In our present work, the PID controller, helps to minimize the torque ripples in the motor.

The BLDC motor rotor is made of permanent magnet and can vary from 2 to 8 pole pairs with alternate North (N) and South (S) poles. The magnetic material is decided based on magnetic field density. Ferrite magnets, rare earth materials like Neodymium (Nd), Samarium Cobalt (SmCo) and the alloy of Neodymium, Ferrite and Boron (NdFeB) are some examples of rare earth alloy magnets are used to make the permanent magnet pole pieces[17],[18]. The position of the motor while rotating can be determined with the help of hall effect sensor and quadratic axis encoder also called as rotary encoder. For low cost application the hall sensor is used, which can be found inside the stator on the driving end. Generally, 3 hall effect sensors are mounted at 120° angle apart from each other. Whenever the magnetic poles pass the hall sensors give out a signal, high indicating North and low indicating South. Based on the combination of these 3 hall effect sensors, the position of motor is determined. Thereby the speed of the motor is being monitored and controlled by using closed loop feedback control mode of operation. The working principle of brushless DC motors is the same as regular DC motor, the Lorentz law, which states that a current carrying conductor placed in a magnetic field experiences a force. This, in turn generates an equally opposite reaction force on the magnet. In BLDC motor, the current carrying conductor stays stationary while the permanent magnet rotates. In practical operation of the 3phase BLDC motor, it operates in a 2-phase active fashion, i.e. energizing the two phases producing the highest torque while keeping the third phase inactive [19]. Energization of the two phases depends on the rotor position i.e. each sequence has current flowing into one

winding (positively energized), current flowing out of one winding (negatively energized) and one winding non-energized. This principle of operation is due to the star winding of the stator present to energize the coils. And to complete one electrical cycle, it generally takes 6 steps of operation. However, electrical cycle is not equal to mechanical revolution. The rotor pole pairs sets base for the amount of electrical cycles to be repeated in order to complete a mechanical rotation. For each rotor pole pairs, one electrical cycle is completed. So, the mechanical revolution (rpm) is one half of the electrical revolution times the number of poles.

Based on the previous work of research work related to the speed control of the BLDC motor, a comparative table of research work conclude that the PID controller is suitable for sinusoidal PWM technique, as described in table 1. The motor speed is being controlled by mechanical revolution. Based on the desired input from the driver to run at the rpm, the PID controller controls the PWM signals. And the controlled signals are being sent to the inverter for the switching the switches. The inverter converts DC power from the battery into the AC power with the helpof these switches. And the sequences of operation of each switch are based rotor position.

**Table 1**. Comparison of Control Strategies for BLDC motor.

| Control Logic and Methodology | Outcome | Ref. No. |
|---|---|---|
| **PID controller with sing Adaptive Fuzzy controller** | In this method, in addition to the Fuzzy PID control process, an adaptive process of normalizing the inputs and outputs of the fuzzy controller is employed. This puts a cap on the error obtained and provides slightly finer results under certain operating conditions. | [3] |
| **PI with SPWM and SVPWM** | With SVPWM technique, the system performance is enhanced, motor requires lesser current, speed response is smoothened and torque ripple is pretty much flattened. | [13] |
| **PI and Fuzzy** | PI with Fuzzy is better over conventional PI with faster steady state speed and lesser torque ripple | [20] |
| **PI with Sensorless FOC** | Phase locked loop and back EMF used to estimate position with minute angular position error and peak to peak estimation error. | [21] |
| **PI with SPWM and SVPWM** | Under normal operating conditions, both techniques are on par with each other. SVPWM however, gives a higher power output thus providing a bit better performance. | [22] |
| **FOC with dither signal** | Dither signal injection quench the limit cycles appearing in the system caused by non-linearity, thereby reducing the overall torque ripple and improving the response of FOC | [23] |
| **PI with FOC, SFOC & Hysteresis** | SFOC shows the least torque ripple out of the three methods | [24] |

## 2. BLDC Motor Control

BLDC motor control is carried out with mathematical model of the BLDC motor, and then implementation of controller [25] [26],[27]. The mathematical model is developed with the idea of state space system design wherein using the state variables, state-space models describe a system through a set of differential or difference equations [28]. And the model is developed using continuous-time representation. The controller is used for controlling this developed model of BLDC motor [29],[30]. The controller regulates the actual speed with regards to the reference speed, thereby reducing the error percentage in overshoot, undershoot, and torque ripple. These problems in the controller can be minimized by using the optimum control strategy. Based on our literature review of various control strategies, the PID control with SVPWM is the best method, through which the system performance is enhanced, motor requires lesser current, speed response is smoothened and torque ripple is pretty much flattened.

### *2.1. Mathematical Model of the 3 – Phase BLDC Motor*

The modelling of the BLDC motor is based on assumption:

- Balanced three phase connections
- The loss in the variable load like stray and copper losses are assumed to be negligible and loss in the constant load like hysteresis and eddy current losses are also neglected while modelling
- There is uniform air gap is maintained between the stator and the rotor
- The switches used in the inverter are considered to be operated at ideal condition, neglecting losses inside them.
- The internal resistances of the three phase stator winding are considered to be equal.
- The value of inductance are assumed to be constant, where self and mutual inductance are considered equal

The motor parameters that are used for modeling are explained in the appendix in the later section.[31][32] The Mathematical model of the armature winding of the BLDC motor is expressed in the form of equation (1) to equation (7).

$$V_{an} = Ri_a + \frac{d(\lambda_a)}{dt} + e_{an} \quad (1)$$

$$V_{bn} = Ri_b + \frac{d(\lambda_b)}{dt} + e_{bn} \quad (2)$$

$$V_{cn} = Ri_c + \frac{d(\lambda_c)}{dt} + e_{cn} \quad (3)$$

$$\lambda_a = L_s i_a - M(i_b + i_c) = L_s . i_a + M(i_a) = (L_s + M).i_a \quad (4)$$

$$\lambda_b = L_s i_b - M(i_a + i_c) = L_s . i_b + M(i_b) = (L_s + M).i_b \quad (5)$$

$$\lambda_c = L_s i_c - M(i_a + i_b) = L_s . i_c + M(i_c) = (L_s + M).i_c \quad (6)$$

Thus these equations can be represented in this form of matrix, where p is $\frac{d}{dt}$.

$$\begin{bmatrix} V_{an} \\ V_{bn} \\ V_{cn} \end{bmatrix} = \begin{bmatrix} R + p(L+M) & 0 & 0 \\ 0 & R + p(L+M) & 0 \\ 0 & 0 & R + p(L+M) \end{bmatrix} \begin{bmatrix} i_a \\ i_b \\ i_c \end{bmatrix} + \begin{bmatrix} e_{an} \\ e_{bn} \\ e_{cn} \end{bmatrix} \quad (7)$$

As the BLDC motor rotates, each winding generates a voltage known as back EMF, which opposes the supply voltage, according to Lenz's law. The polarity of the back EMF is opposite to the supply voltage and is dependent on the rotor position. The systematical order of equations that are being used in the BLDC are explained below. As the system is a multi input multi output, the traditional state space form of representation cannot be used, as the differential term is used. Thus using these equations, the complete mathematical model of BLDC motor is modeled using Matlab / Simulink, as shown in figure 1.

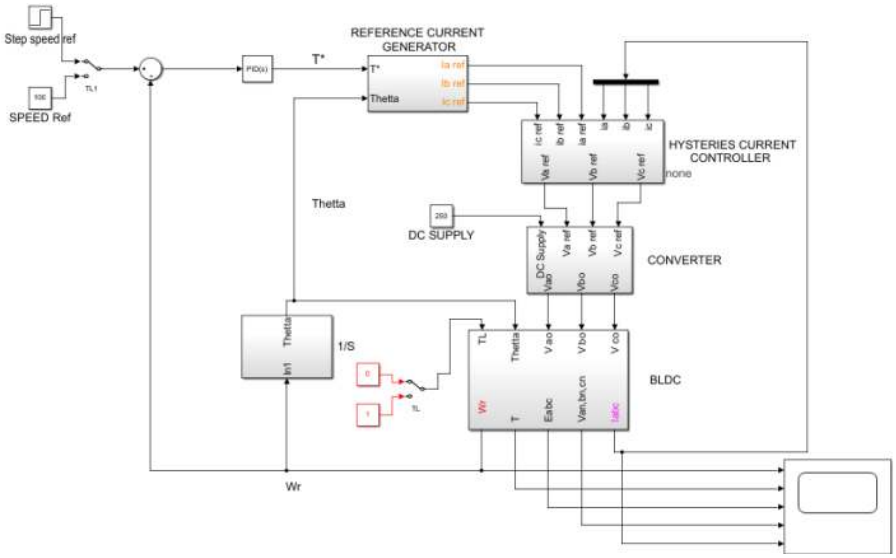


**Figure 1.** MATLAB Simulink model for BLDC motor Control.

*2.1.1. Voltage Measurement*

Using the following equation (8) the phase voltage across the terminals of the motors is determined. And as the BLDC motor has no neutral connection, equation (9) is used. Thus using these two equations the voltage across each phase is determined using equation (11) to equation (13).

$$V_{ao} + V_{bo} + V_{co} - 3V_{no} = R(i_a + i_b + i_c) + (L_s + M)\left(\frac{d(i_a)}{dt} + \frac{d(i_b)}{dt} + \frac{d(i_c)}{dt}\right) + e_{an} + e_{bn} + e_{cn} \quad (8)$$

$$i_a + i_b + i_c = 0 \quad (9)$$

$$V_{no} = \frac{1}{3}\{(V_{ao} + V_{bo} + V_{co}) - (e_{an} + e_{bn} + e_{cn})\} \quad (10)$$

$$V_{an} = V_{ao} - V_{no} \quad (11)$$

$$V_{bn} = V_{bo} - V_{no} \quad (12)$$

$$V_{cn} = V_{co} - V_{no} \quad (13)$$

*2.1.2. Current Measurement*

From equation (1) the relationship between the voltage and the current equations is being obtained. And, upon integration of the equation (14), the value of current across each phase of the stator of the BLDC motor is obtained. Similarly, different block is used to find the current at different phases$i_a$, $i_b$ and $i_c$ [33].

$$\frac{d(i_a)}{dt} = \frac{(V_{an} - R.i_a - e_{an})}{(L_s + M)} \quad (14)$$

*2.1.3. Electromagnetic Torque Measurement*

The electromagnetic torque, which has a unit of N-m, is measured using the help of the equation (15). Normalized Back EMF function,$f_a(\theta_r)$, $f_b(\theta_r)$ and $f_c(\theta_r)$ are trapezoidal function. Thus from equation (15) to equation (17), the generalized electromagnetic torque equation is determined. And using the help of the supporting equation (15) to equation (17), the final electromagnetic equation is determined using equation (19).

$$T_e = \{(e_{an}i_a) + (e_{bn}i_b) + (e_{cn}i_c)\}/(\omega_r) \quad (15)$$

$$e_{an} = E\, f_a(\theta_r), e_{bn} = E\, f_b(\theta_r), e_{cn} = E\, f_c(\theta_r) \quad (16)$$

$$E = K_b\omega_r \quad (17)$$

$$T_e = \frac{(E.f_a(\theta_r).i_a) + (E.f_b(\theta_r).i_b) + (E.f_c(\theta_r).i_c)}{\omega_r} \quad (18)$$

$$T_e = K_b.\{f_a(\theta_r).i_a + f_b(\theta_r).i_b + f_c(\theta_r).i_c\} \quad (19)$$

*2.1.4. Angular Velocity Measurement*

The general torque equation for the rotating objects is expressed in equation (20), and upon simplification with the help of equation(21) the final angular velocity measurement is obtained using equation (22). [34]

$$J\frac{d\omega}{dt} + B.\omega = T_e - T_l \quad (20)$$

$$\omega_r = \omega\,.\frac{P}{2} \quad (21)$$

$$\frac{d\omega_r}{dt} = \frac{P}{2}\left(\frac{T_e - T_l - B.\omega_r}{J}\right) \quad (22)$$

*2.1.5. Creation of Back EMF (Trapezoidal Function)*

Based on the angle of rotation $\boldsymbol{\theta}_r$, the value of the normalized back EMF is taken out using the look up table in the Matlab environment, as shown in table 2.

**Table 2**. Logic for Look up table for rotor position.

| **Rotor Position Signal** | | **Normalized Back EMF** | |
|---|---|---|---|
| **θr** | **$e_{an}$** | **$e_{bn}$** | **$e_{cn}$** |
| 0° - 60° | E | −E | (6E/π)(π-θr) -E |
| 60° - 120° | E | (6E/π)(θr-2π) +E | −E |
| 120° -180° | (6E/π)(π-θr) -E | E | −E |
| 180° - 240° | −E | E | (6E/π)(θr-2π) +E |
| 240° - 300° | −E | (6E/π)(π-θr) -E | E |
| 300° - 360° | (6E/π)(θr-2π) +E | −E | E |

*2.2. Mathematical Model of Hysteresis Current Controller and Reference Current Generator*

The reference current controller takes in the input of the controller. The controller gives the required torque for the corresponding input. It uses look up table as shown in table 3, to find the reference current $i_a$, $i_b$ and $i_c$ (reference) response, based on the theta (angular position) response of the motor [35],[36],[37]. The hysteresis current controller is one of the current control strategies to control the inverter. While modeling it, a relay is used for generating the square pulses, as shown in figure 2, where the switch on point is 0.01, switch off point is -0.01. Output from the generator is on when its value 1 and the output is off when its value is -1.

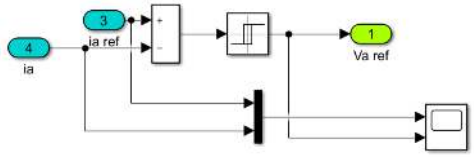


**Figure 2**. Reference Current model

**Table 3**. Look-up table for 3 phases of current.

| **Rotor Position Signal** | **Reference Currents (amps)** | | |
|---|---|---|---|
| **θ r (deg)** | **Ia** | **Ib** | **ic** |
| 0° - 60° | I∗ | −I∗ | 0 |
| 60° - 120° | I∗ | 0 | −I∗ |
| 120° -180° | 0 | I∗ | −I∗ |
| 180° - 240° | −I∗ | I∗ | 0 |
| 240° - 300° | −I∗ | 0 | I∗ |
| 300° - 360° | 0 | −I∗ | I∗ |

*2.3. Mathematical Model of the 3-Phase BLDC Motor with FOC using Space Vector Pulse Width Modulation (SVPWM)*

SVPWM is a technique used in FOC control, to determine the pulse-width modulated (PWM) signals for the inverter switches in order to generate the desired 3-phase voltage supply to the motor. Here the 3 phase current ($i_a$, $i_b$ and $i_c$)is converted into 2 phase ($i_d$, $i_q$) by using park transform, as shown in equation (23). The frequency domain is converted into time domain here. This is done with respect to

the rotating reference frame, here motor rotation angle is considered as the rotating frame. Then the PI controller is used for stabilizing the current in the d and q axis.

$$\begin{bmatrix} d \\ q \\ 0 \end{bmatrix} = \frac{2}{3}\begin{bmatrix} \sin(\theta) & \sin(\theta - \frac{2\pi}{3}) & \sin(\theta + \frac{2\pi}{3}) \\ \cos(\theta) & \cos(\theta - \frac{2\pi}{3}) & \cos(\theta + \frac{2\pi}{3}) \\ 1/2 & 1/2 & 1/2 \end{bmatrix}\begin{bmatrix} a \\ b \\ c \end{bmatrix} \tag{23}$$

The error for the PI controller of q axis is taken as the difference between the input of the speed controller and actual magnitude of value of $I_d$, and the error for the PI controller of d axis is taken as the difference of reference $I_d$ as 0, and the actual $I_d$. Since the d axis current is the key component for torque production, this process of setting 0 as the reference helps in reducing the torque ripple from the BLDC motor. The conversion of the reference $I_d$ and $I_q$ currents into α and β axis currents need to be carried out for simplification of mathematical representation. As the SVPWM requires the α and β axis as the input for generating switching pattern. Hence inverse park transform is being used here. Where $I_\alpha$ and $I_\beta$, the angle between them is determined as shown in equation (24), and the sector is allocated according to the angle. Using this approach the mathematical model was developed as shown in figure 3.

$$\begin{bmatrix} I_\alpha \\ I_\beta \end{bmatrix} = \begin{bmatrix} \cos(\theta) & -\sin(\theta) \\ \sin(\theta) & \cos(\theta) \end{bmatrix}\begin{bmatrix} I_d \\ I_q \end{bmatrix} \tag{24}$$

The total number of possible switch configurations is $2^3$=8. Where, the 6 of these configurations (001,011,010,110,100,101) correspond to different voltages, called as the basic vector. And the last two (000,111) are referred to as zero vector, as they represent zero volts on the terminals. Where 0 represent off state of switch and 1 represent on state of switch.

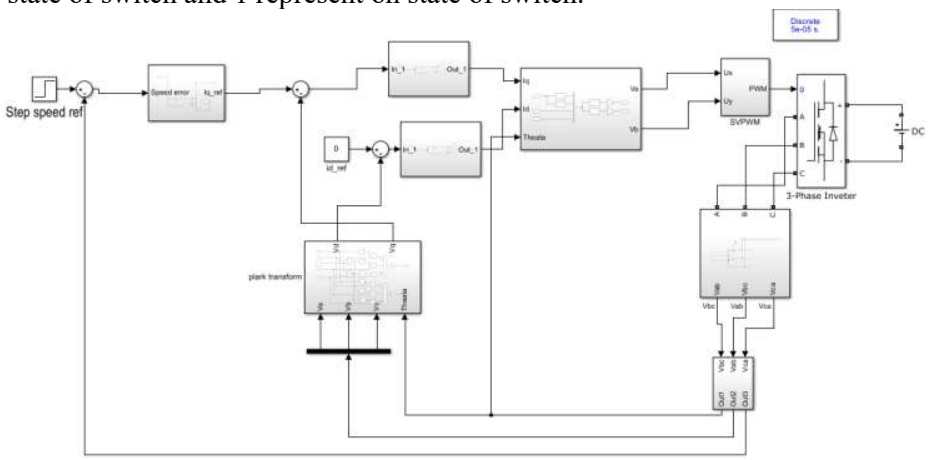


**Figure 3**. FOC with SVPWM Simulink Model.

Now based on the sector, $I_\alpha$ and $I_\beta$, the timing for each sector is determined using the Matlab function in the simulink environment. The switching frequency of the switches is kept 10 kHz. And the switching period is ΔT = 0.0001 sec. The geometric summation from the figure 4 corresponding to the phase angle, can be expressed as shown in equation (25), where $T_{sv1}$ and $T_{sv2}$ are the time period during which space vector $SV_1$ and $SV_2$ are selected respectively. They can be expressed in cartesian form as shown in equation (26).

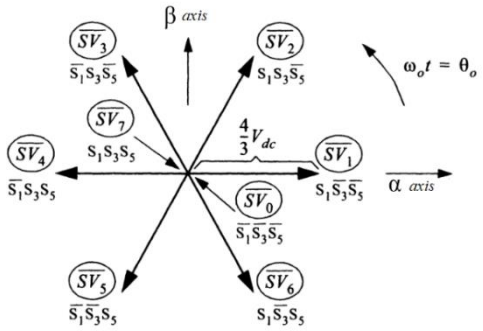


**Figure 4**. Space Vector Diagram.

$$V_o < \theta_o = \frac{T_{SV1}}{\Delta T/2} SV_1 + \frac{T_{SV2}}{\Delta T/2} SV_2 \tag{25}$$

$$V_o \left(\cos(\theta_o) + \boldsymbol{j} * \sin(\theta_o)\right)\frac{\Delta T}{2} = T_{SV1}V_m + T_{SV2}V_m\left(\cos\left(\frac{\pi}{3}\right) + \mathbf{j} * \mathbf{s}\sin\left(\frac{\pi}{3}\right)\right) \tag{26}$$

**Table 4**. Equations for Space Vector Control.

| $\boldsymbol{\omega_0 t = \theta_0}$ **(deg)** | Space Vector with Active Times |
|---|---|
| **0° - 60°** | $T_{SV1} = \frac{V_0}{V_{dc}}\frac{\sqrt{3}}{2}\cos\left(\theta_0 + \frac{\pi}{6}\right).\frac{\Delta T}{2}$ |
| | $T_{SV2} = \frac{V_0}{V_{dc}}\frac{\sqrt{3}}{2}\cos\left(\theta_0 - \frac{\pi}{2}\right).\frac{\Delta T}{2}$ |
| **60° - 120°** | $T_{SV2} = \frac{V_0}{V_{dc}}\frac{\sqrt{3}}{2}\cos\left(\theta_0 - \frac{\pi}{6}\right).\frac{\Delta T}{2}$ |
| | $T_{SV3} = \frac{V_0}{V_{dc}}\frac{\sqrt{3}}{2}\cos\left(\theta_0 - \frac{5\pi}{6}\right).\frac{\Delta T}{2}$ |
| **120° -180°** | $T_{SV3} = \frac{V_0}{V_{dc}}\frac{\sqrt{3}}{2}\cos\left(\theta_0 + \frac{\pi}{2}\right).\frac{\Delta T}{2}$ |
| | $T_{SV4} = \frac{V_0}{V_{dc}}\frac{\sqrt{3}}{2}\cos\left(\theta_0 - \frac{7\pi}{6}\right).\frac{\Delta T}{2}$ |
| **180° - 240°** | $T_{SV4} = \frac{V_0}{V_{dc}}\frac{\sqrt{3}}{2}\cos\left(\theta_0 - \frac{5\pi}{6}\right).\frac{\Delta T}{2}$ |
| | $T_{SV5} = \frac{V_0}{V_{dc}}\frac{\sqrt{3}}{2}\cos\left(\theta_0 - \frac{3\pi}{2}\right).\frac{\Delta T}{2}$ |
| **240° - 300°** | $T_{SV5} = \frac{V_0}{V_{dc}}\frac{\sqrt{3}}{2}\cos\left(\theta_0 - \frac{7\pi}{6}\right).\frac{\Delta T}{2}$ |
| | $T_{SV6} = \frac{V_0}{V_{dc}}\frac{\sqrt{3}}{2}\cos\left(\theta_0 - \frac{11\pi}{6}\right).\frac{\Delta T}{2}$ |
| **300° - 360°** | $T_{SV6} = \frac{V_0}{V_{dc}}\frac{\sqrt{3}}{2}\cos\left(\theta_0 - \frac{3\pi}{2}\right).\frac{\Delta T}{2}$ |
| | $T_{SV1} = \frac{V_0}{V_{dc}}\frac{\sqrt{3}}{2}\cos\left(\theta_0 - \frac{\pi}{6}\right).\frac{\Delta T}{2}$ |

On equating the real and imaginary parts, the solution of $T_{SV1}$ and $T_{SV2}$ is obtained. The table 4 shows the arbitrary target output for any phase angle, which was created from the two closest space vector components. Therefore, along with relevant expressions, these define the active time intervals

for each space vector. Based on these time intervals the active pulse duration is determined and is then compared with a repeating sequence to generate the PWM waveform, which sends the supply pulses to the inverter.The inverter converts DC to AC supply, as the BLDC motor is an AC motor. Based on the switching pulses sequence the output waveform of AC supply is generated. This voltage is directly fed into the motor, for the efficient operation of the motor. As the switches in the inverter at bottom section operates exactly opposite in supply to the top section. And as the top section consists of 3 switches and bottom section consists of 3 switches for the 3 phase 2 level inverter.When the load on the motor is of unpredictable nature, as in case of Electric Vehicle (EV) the supply current from the battery keeps varying, which increases the THD. And if this parameter increases, the torque ripple increases. This is the only limitation of this mode of operation.

### *2.4. Total Harmonic Distortion (THD)*

Harmonics or harmonic frequencies of a periodic voltage or current are frequency components in the signal that are at integer multiples of the frequency of the main signal. This is the basic outcome that fourier analysis of a periodic signal shows. Harmonic distortion is the distortion of the signal due to these harmonics.

A voltage or current that is purely sinusoidal has no harmonic distortion because it is a signal consisting of a single frequency. A voltage or current that is periodic but not purely sinusoidal will have higher frequency components in it contributing to the harmonic distortion of the signal. In general, the less that a periodic signal looks like a sine wave, the stronger the harmonic components are and the more harmonic distortion it will have. So, a purely sinusoidal signal has no distortion while a square wave, which is periodic but does not look sinusoidal at all, will have lots of harmonic distortion. In the real world, of course, sinusoidal voltages and currents are not perfectly sinusoidal; some amount of harmonic distortion will be present. Figure 5 provide visual comparisons, in the time domain and the frequency domain, of a sinusoidal voltage and a square wave voltage.THD could be defined as ratio of the RMS voltage of all the harmonic frequencies (from the 2nd harmonic on) over the RMS voltage of the fundamental frequency (the fundamental frequency is the main frequency of the signal, i.e., the frequency that you would identify if examining the signal with an oscilloscope) as shown in equation (27) and equation (28).

$$\mathrm{THD} = \frac{\sum_{n=2}^{\infty} V_{n\_rms}^2}{V_{fundamental\_rms}} \tag{27}$$

$$vsquare\,(t) = \left(\frac{4}{\pi}\right)\sin(2\pi ft) + \left(\frac{4}{3\pi}\right)\sin(6\pi ft) + \left(\frac{4}{5\pi}\right)\sin(10\pi ft) + \cdots + \left(\frac{4}{n\pi}\right)\sin(2n\pi ft) \tag{28}$$

THD is important in several types of systems, including power systems, where a low THD means higher power factor, lower peak currents, and higher efficiency; audio systems, where low THD means that the audio signal is a more faithful reproduction of the original recording; and communication systems, where low THD means less interference with other devices and higher transmit power for the signal of interest. Generally the EV is a miniature power system, it has various audio-video instruments and network connectivity, therefore or this system, the lower the THD, better the power factor and lower is the interference with the system.

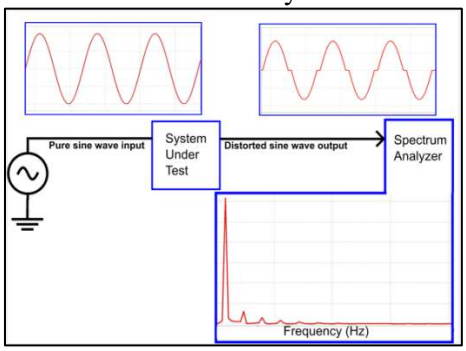


**Figure 5**. System that introduces crossover distortion into a signal.

### *2.5. Tuning of PID Controller*

The designed plant is so complicated that its mathematical model cannot be easily obtained, therefore the experimental approaches to tune the PID controller is carried out. By varying the proportional gain ($K_p$), integral time ($T_i$) and derivative time ($T_d$) to different values, the optimal value has been estimated. This optimal value is based on the desired output from the system. For EV applications, the rise time and the settling time should be as minimum as possible, so the desired speed from the throttle to the wheel, is achieved as quick as possible. And the overshoot percentage should not be too high, as it creates sudden load to the drive wheel, which decreases the life cycle of the power train. The general layout for plant system using PID control is shown in figure 6.

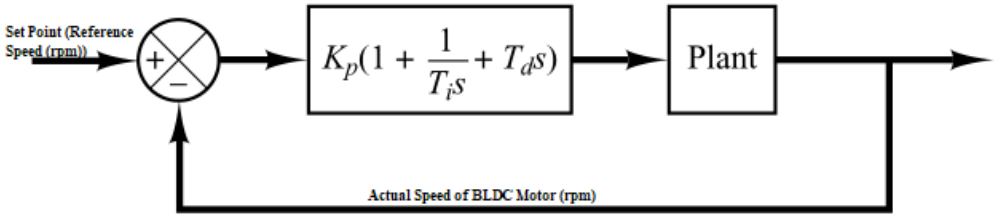


**Figure 6**. PID Control Loop for the model.

While tuning the following observations was noted down like, as the value of $K_p$, increased, the rise time decreases, the overshoot increases, and settling time is not having much influence. Similarly, with the increase the value of $T_i$, the rise time decreases, the overshoot increases, and settling time increases. Similarly, when $T_d$ increases, the rise time increases, overshoot decreases and settling time decreases. By trying different iterations, the optimal value of the gains was determined, as showed in table 5.

**Table 5**. PID Tuning for finding optimum gain values for the PID Controller of the BLDC motor.

| Sl. No. | Kp | Ti | Td | Rise Time (ms) | Over shoot(%) | Settling Time (ms) |
|---|---|---|---|---|---|---|
| **1** | 0.4 | 6 | 0 | 26.747 | 26.747 | 186.701 |
| **2** | 0.5 | 7 | 0.00001 | 22.643 | 3.716 | 120 |
| **3** | 0.5 | 4 | 0.0001 | 41.804 | 1.622 | 205.496 |
| **4** | 0.5 | 4 | 0.001 | 51.613 | 1.183 | 120.327 |
| **5** | 0.5 | 4 | 0.01 | 92.612 | 1.482 | 272.247 |
| **6** | 0.4 | 4 | 0.01 | 85.676 | 3.55 | 317.905 |
| **7** | 1 | 4 | 0.04 | 109.04 | 0.5 | 174.108 |
| **8** | 0.6 | 4 | 0.01 | 59.691 | 3 | 275.863 |
| **9** | 0.8 | 7 | 0.001 | 25.444 | 1.05 | 174.042 |
| **10** | 0.9 | 8 | 0.001 | 23.669 | 2.5 | 221.19 |
| **11** | 0.8 | 6 | 0.001 | 26.063 | 1.2 | 167.721 |
| **12** | 0.8 | 8 | 0.001 | 22.366 | 1.006 | 110.482 |

## 3. Results and Discussion

### *3.1. Tuning of PID Controller*

The input was given as step response of 100 to 150 rpm. Then the error from this reference to the actual speed of the motor is given as the feed to the PID controller. Then the controller sends the optimal signal to the reference current generator, to send the optimal current supply to the inverter, with the help of PWM technique the pulse width is being controlled for regulating the speed of the motor. The Sinusoidal PWM technique sends the signals to the inverter, which in turn sends the

voltages, $V_a$, $V_b$ and $V_c$ to the motor. Then the actual speed of the motor is compared with the reference speed for minimization of error as shown in figure 7. Based on experiment when the Proportional gain as 0.8, integral gain as 8 and derivative gain as 0.001. the rise time is 22ms, overshoot is 1% and settling time is 110ms. These optimal gains can be directly implemented into the motor controller.

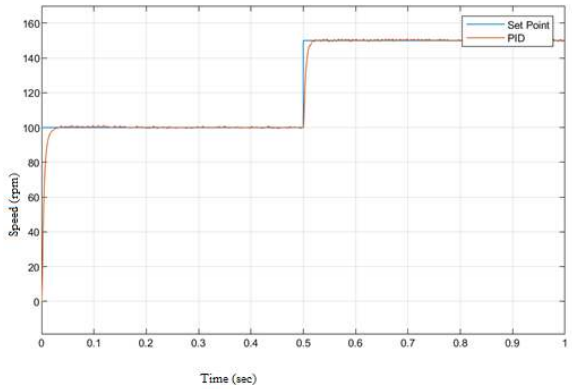


**Figure 7**. Speed Response chart of motor after PID tuning.

*3.2. Reduction of THD*

Based on the comparison between different types of control strategy used for controlling the speed of the motor, when the predefined parameters are fundamental frequency is 60 Hz, switching frequency of the inverter is 10kHz. The figure 8 shows the Total harmonic distortion of the supply current of phase A. And the value of the THD was found minimum for the SVPWM technique.

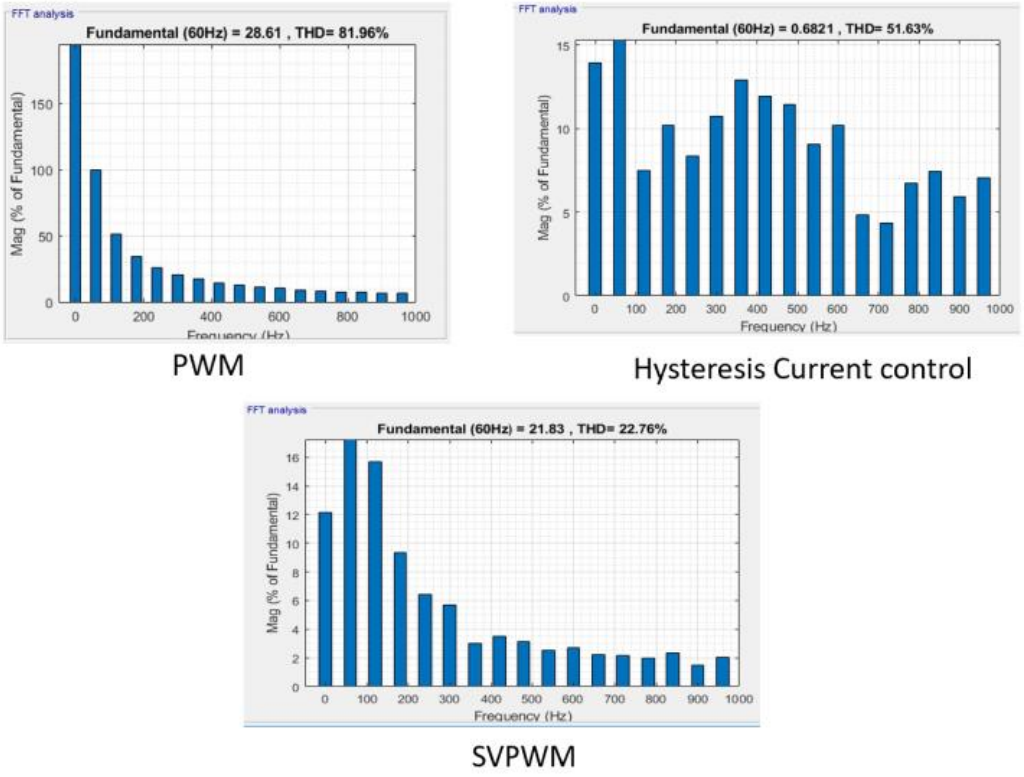


**Figure 8**. Clockwise from top left: PWM control based on Hall sensor, Hysteresis control and SVPWM control with FOC, SVPWM control with FOC.

## 4. Future Scope of Implementation of PID with Modified SVPWM Control in DSPACE Controller

Using the DSPACE MicroLabBox version 1202, the control of the speed of the BLDC motor can be carried out. Using the help of Real Time Interface (RTI) tool block which is present inside the Matlab Simulink Environment as shown in figure 9. The model in the Simulink environment was carried out, but it couldn't be tested, due to time constraint to visualize the results. [38],[39],[40],[41]

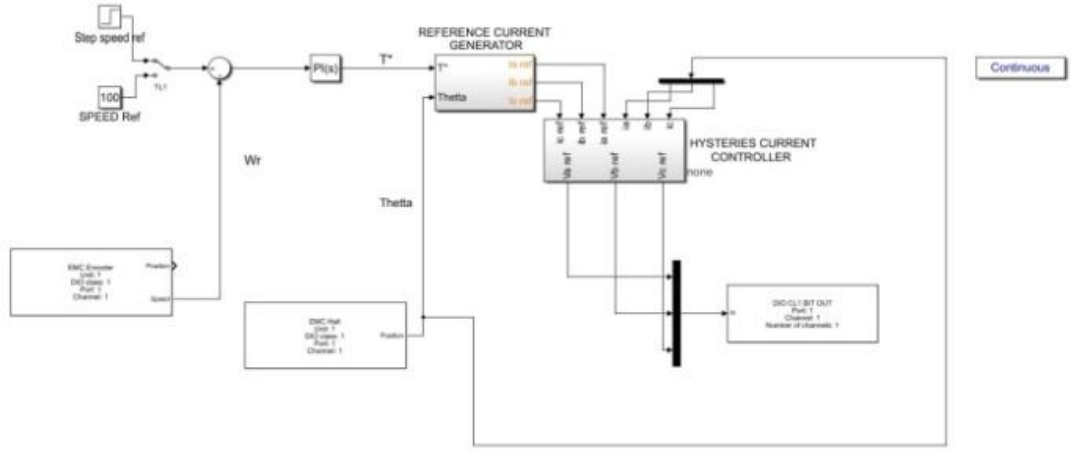


**Figure 9.** BLDC motor model integrated with the D-space controller to control the hardware directly with MATLAB.

## 5. Appendices

### *5.1. Motor Parameters used for Modelling*

The constants that are used in the mathematical modelling of the BLDC motor using MATLAB / Simulink was developed according to the table 6 and table 7.

**Table 6**. Motor Parameters used for Modelling

| Parameters | Value | Units | Description |
|---|---|---|---|
| **Kb** | 1.23 | (const.) | Field Flux due to permanent magnet of Rotor (Ferrite Magnet, rare earth alloys are used to make the permanent magnet pole pieces) |
| **J** | 0.013 | Kg – $m^2$ | Equivalent Moment of Inertia of Motor and Load on Motor shaft |
| **P** | 4 | (const.) | Number of Poles of Rotor (can vary from 2 to 8 poles) |
| **R** | 2.8 | Ohm | Resistance of stator winding |
| **Ls + M** | 0.00521 | Hendry | Inductance (M - Mutual inductance and $L_s$ -Self-inductance) |
| **B** | 0.005 | N-m-s/rad | Damping Co-efficient |
| **DC power Supply** | 250 | volts | Applied Voltage |

*5.2. Notations used in this paper*

**Table 7.** Notations used in this paper.

| Symbol | Units | Meaning |
|---|---|---|
| **Ra,Rb, Rc** | Ohm | Stator Resistance of phase A, B, C |
| **La, Lb, Lc** | Hendry | stator inductance of phase A, B, C |
| **Van, Vbn, Vcn** | Volt | Stator voltage in phase A.B,C |
| **ia, ib, ic** | Ampere | Stator Current in phase A, B,C |
| **ean, ebn, ecn** | volt | Back EMF in phase A,B, C |
| **ωr** | rad/sec | Rotor speed in electrical |
| **ω** | Rad/sec | Mechanical rotor speed |
| $\boldsymbol{\lambda a, \lambda b, \lambda c}$ | | flux linkage of phase windings a, b and c |

## 6. References

[1] Devi, K. S., Dhanasekaran, R., & Muthulakshmi, S., 2016, May. Improvement of speed control performance in BLDC motor using fuzzy PID controller. In *2016 International Conference on Advanced Communication Control and Computing Technologies (ICACCCT)* (pp. 380-384). IEEE.

[2] Shanmugasundram, R., Zakariah, K. M., & Yadaiah, N. 2012, November. Implementation and performance analysis of digital controllers for brushless DC motor drives. IEEE/ASME transactions on mechatronics, 19(1), 213-224.

[3] Crnosija, P., Krishnan, R., & Bjazic, T. 2006, Optimization of PM brushless DC motor drive speed controller using modification of Ziegler-Nichols methods based on Bodé plots. In *2006 12th International Power Electronics and Motion Control Conference* (pp. 343-348). IEEE..

[4] Suganthi, P., Nagapavithra, S. and Umamaheswari, S., 2017, March. Modeling and simulation of closed loop speed control for BLDC motor. In *2017 Conference on Emerging Devices and Smart Systems (ICEDSS)* (pp. 229-233). IEEE.

[5] Chougale, R.G. and Lakade, C.R., 2017, September. Regenerative braking system of electric vehicle driven by brushless DC motor using fuzzy logic. In *2017 IEEE International Conference on Power, Control, Signals and Instrumentation Engineering (ICPCSI)* (pp. 2167-2171). IEEE.

[6] Varshney, A., Gupta, D. and Dwivedi, B., 2017. Speed response of brushless DC motor using fuzzy PID controller under varying load condition. *Journal of Electrical Systems and Information Technology*, *4*(2), pp.310-321.

[7] Kandiban, R. and Arulmozhiyal, R., 2012. Speed control of BLDC motor using adaptive fuzzy PID controller. *Procedia Engineering*, *38*, pp.306-313.

[8] Krishnan, P.H. and Arjun, M., 2014, March. Control of BLDC motor based on adaptive fuzzy logic PID controller. In *2014 International Conference on Green Computing Communication and Electrical Engineering (ICGCCEE)* (pp. 1-5). IEEE.

[9] Xuanfeng, S. and Xingyan, L., 2010, October. BLDC motor speed servo system based on novel P-fuzzy self-adaptive PID control. In *2010 International Conference on Information, Networking and Automation (ICINA)* (Vol. 2, pp. V2-186). IEEE.

[10] Kwon, C.J., Han, W.Y., Kim, S.J. and Lee, C.G., 2003, August. Speed controller with adaptive fuzzy tuning for BLDC motor drive under load variations. In *SICE 2003 Annual Conference (IEEE Cat. No. 03TH8734)* (Vol. 3, pp. 3118-3121). IEEE.

[11] Milani, M.M.R.A., Çavdar, T. and Aghjehkand, V.F., 2012, July. Particle swarm optimization—based determination of Ziegler-Nichols parameters for PID controller of brushless DC motors. In *2012 International Symposium on Innovations in Intelligent Systems and Applications* (pp. 1-5). IEEE.

[12] Irimia, N.D., Lazar, F.I. and Luchian, M., 2019, April. Comparison between sinusoidal and

space vector modulation techniques on the resulting electromagnetic torque ripple produced by a three-phase BLDC motor under field-oriented control. In *2019 6th International Conference on Control, Decision and Information Technologies (CoDIT)* (pp. 640-645). IEEE.

[13] Gujjar MN, Kumar P. Comparative analysis of field oriented control of BLDC motor using SPWM and SVPWM techniques. In2017 2nd IEEE International Conference on Recent Trends in Electronics, Information & Communication Technology (RTEICT) 2017 May 19 (pp. 924-929). IEEE.

[14] Holmes DG, Lipo TA. Pulse width modulation for power converters: principles and practice. John Wiley & Sons; 2003 Oct 3.

[15] Kang SJ, Sul SK. Direct torque control of brushless DC motor with nonideal trapezoidal back EMF. IEEE Transactions on power electronics. 1995 Nov;10(6):796-802.

[16] Xintong, J., Jingwei, X., Yong, L. and Yongping, L., 2009. Theoretical and simulation analysis of influences of stator tooth width on cogging torque of BLDC motors. *IEEE Transactions on Magnetics*, *45*(10), pp.4601-4604.

[17] Whiteley E, inventor; Maghemite Inc, assignee. Brushless DC dynamoelectric machine having ferrite material magnetic circuit. United States patent US 4,605,874. 1986 Aug 12.

[18] Qu R, Aydin M, Lipo TA. Performance comparison of dual-rotor radial-flux and axial-flux permanent-magnet BLDC machines. InIEEE International Electric Machines and Drives Conference, 2003. IEMDC'03. 2003 Jun 1 (Vol. 3, pp. 1948-1954). IEEE.

[19] Rashid MH, editor. Power electronics handbook. Butterworth-Heinemann; 2017 Sep 9.

[20] Sharma, Pragati K., and A. S. Sindekar. 'Performance Analysis and Comparison of BLDC Motor Drive using PI and FOC', IEEE 2016 *International Conference on Global Trends in Signal Processing, Information Computing and Communication (ICGTSPICC)*, 2016 Dec 22, (pp. 485-492).

[21] de Almeida, T. E., de Paula, G. T., de Castro, A. G., Pereira, W. C., & José, R. D. A. 2017, November. Sensorless vector control for BLDC machine. In *2017 Brazilian Power Electronics Conference (COBEP)* (pp. 1-6). IEEE.

[22] Chen, S.C. and Mbitu, E.T., 2018, April. Permanent magnet brushless motor field oriented control with dither signal injection. In *2018 IEEE International Conference on Applied System Invention (ICASI)* (pp. 1141-1144). IEEE.

[23] Kumar, B.P. and Krishnan, C.M.C., 2016, January. Comparative study of different control algorithms on brushless DC motors. In *2016 Biennial International Conference on Power and Energy Systems: Towards Sustainable Energy (PESTSE)* (pp. 1-5). IEEE.

[24] Ogata K, Yang Y. Modern control engineering. Upper Saddle River, NJ: Prentice hall; 2010 Sep.

[25] Wongkhead S, Tunyasrirut S, Permpoonsinsup W, Puangdownreong D. Simulation and Analysis of Speed Brushless Direct Current Motor Based on State Space Modeling. In2018 International Conference on Engineering, Applied Sciences, and Technology (ICEAST) 2018 Jul 4 (pp. 1-4). IEEE.

[26] Singh, C.P., Kulkarni, S.S., Rana, S.C. and Deo, K., 2013. State-space based simulink modeling of BLDC motor and its speed control using fuzzy PID controller. *International Journal of Advances in Engineering Science and Technology*, *2*(3), pp.359-369.

[27] Bondre VS, Thosar AG. Mathematical modeling of direct torque control of BLDC motor. In2017 International Conference on Innovative Research In Electrical Sciences (IICIRES) 2017 Jun 16 (pp. 1-8). IEEE.

[28] Mohankrishna C, Rajesh N, Gowd K, Ramesh A, Gupta GS. Modelling and simulation of BLDC motor using state space approach. International Journal Of Innovative Research In Electrical, Electronics, Instrumentation And Control Engineering. 2016 May;4(5).

[29] Tibor B, Fedak V, Durovský F. Modeling and simulation of the BLDC motor in MATLAB GUI. In2011 IEEE International Symposium on Industrial Electronics 2011 Jun 27 (pp. 1403-1407). IEEE.

[30] Pan, C.T. and Fang, E., 2008. A phase-locked-loop-assisted internal model adjustable-speed controller for BLDC motors. *IEEE Transactions on industrial electronics*, *55*(9), pp.3415-3425.
[31] Rodriguez F, Emadi A. A novel digital control technique for brushless DC motor drives: Conduction-angle control. InIEEE International Conference on Electric Machines and Drives, 2005. 2005 May 15 (pp. 308-314). IEEE.
[32] Jaya A, Purwanto E, Fauziah MB, Murdianto FD, Prabowo G, Rusli MR. Design of PID-fuzzy for speed control of brushless DC motor in dynamic electric vehicle to improve steady-state performance. In2017 International Electronics Symposium on Engineering Technology and Applications (IES-ETA) 2017 Sep 26 (pp. 179-184). IEEE.
[33] Ramesh, M.V., Amarnath, J., Kamakshaiah, S. and Rao, G.S., 2011. Speed control of brushless dc motor by using fuzzy logic pi controller. *ARPN Journal of Engineering and Applied Sciences*, *6*(9), pp.55-62.
[34] Ansari, U. and Alam, S., 2011, March. Modeling and control of three phase BLDC motor using PID with genetic algorithm. In *2011 UkSim 13th International Conference on Computer Modelling and Simulation* (pp. 189-194). IEEE.
[35] Rao, K.S.R. and Othman, A.H.B., 2007, November. Design optimization of a BLDC motor by Genetic Algorithm and Simulated Annealing. In *2007 International Conference on Intelligent and Advanced Systems* (pp. 854-858). IEEE.
[36] Vinodhini, R., Ganesh, C. and Patnaik, S.K., 2012, March. Genetic algorithm optimized on-line neuro-tuned robust position control of BLDC motor. In *2012 IEEE Students' Conference on Electrical, Electronics and Computer Science* (pp. 1-4). IEEE.
[37] Hu, M., Qiu, J. and Shi, C., 2011, August. A comparative analysis of fuzzy PI and PI speed control in Brushless DC motor based on dSPACE. In *2011 International Conference on Electrical Machines and Systems* (pp. 1-5). IEEE.
[38] dSPACE, Implementation Guide For Release 4.0: Real-Time Interface (RTI and RTI-MP). Documentation Guide, August 2003.
[39] dSPACE, Experiment Guide For Release 4.0: Control-Desk. Documentation Guide, August 2003.
[40] Aboulnaga, A.A., Desai, P.C., Rodriguez, F., Cooke, T.R. and Emadi, A., 2004, February. A novel, low-cost, high-performance single-phase adjustable-speed motor drive using PM brush-less DC machine: IIT's design for 2003 future energy challenge. In *Nineteenth Annual IEEE Applied Power Electronics Conference and Exposition, 2004. APEC'04.* (Vol. 3, pp. 1595-1603). IEEE.
[41] Bansal, A. K., Gupta, R. A., & Kumar, R., 2011, January. Fuzzy estimator for sensorless PMBLDC motor drive under speed reversal. In *India International Conference on Power Electronics 2010 (IICPE2010)* (pp. 1-7). IEEE.